Cover-time distribution of random processes in granular gases

Ke Cheng,[1] Jia-Qi Dong,[1] Liang Huang,[1,*] and Lei Yang[2]

[1]*School of Physical Science and Technology and Key Laboratory for Magnetism and Magnetic Materials of MOE, Lanzhou University, Lanzhou, Gansu 730000, China*

[2]*Institute of Modern Physics, Chinese Academy of Science, Lanzhou, Gansu 730000, China*

(Received 24 May 2018; revised manuscript received 27 August 2018; published 3 October 2018)

Random processes have attracted much attention due to their broad applications. Despite the many varieties of random processes, it is proposed that there can be universal properties, e.g., the cover-time distributions for noncompact random walks. In this work, we investigate experimentally the cover-time distribution in random processes of granular gases. In particular, the trajectory of a tracer particle in the granular gases is read out by a high-speed camera, which forms a random process that is specific to granular gas systems. Analysis of the covering process of this trajectory is then carried out to get the cover-time distribution. The direct results of cover-time distribution deviates from the universal law, which can be attributed to two main factors: the attracting effect at the boundary and the nonperiodic boundary condition due to the fixed boundaries. By efficiently removing these effects step by step, the cover-time distribution recovers to the universal law approximately, which also reveals that the attracting effect at the boundary is the most dominant factor leading to the discrepancy. We have carried out three distinct experiments with different granular gas circumstances, and all agreed well with the universal distribution after removing the boundary effects.

DOI: 10.1103/PhysRevE.98.042109

I. INTRODUCTION

Random walk was first proposed by Karl Pearson in 1905 [1], and it has attracted continuous attention for more than 100 years due to the simplicity of the mathematical models and its broad applications in many different disciplines of science [2]. Particularly, in the past few decades, there have been developed more complicated random walk models, such as the Lévy walk [3], persistent random walk [4,5], and self-avoiding random walk [6], etc. Different models typically have distinct diffusion behaviors. However, beyond these different features, there could exist some hidden universal properties among the varieties of random walks, such as the first-passage time distribution [7], the cover-time distribution [8], etc. A straightforward question is how universal are these properties. Are they broadly applicable in realistic random processes or there are certain limitations? In this work we shall try to tackle this problem of cover-time distribution by exploiting the random processes of a tracer particle in a vibrated granular gas environment.

The cover process is that a random walker visits a given set of sites at least once [9]. There is a long history in investigating the cover process of a random walker in a given domain. One of the motivations to investigate the lattice covering problem is to find out how a fractal trajectory fills in higher-dimensional space. There were some early explorations in this interesting problem. The mean cover time has been studied since the 1990s, and analytical expressions have been obtained for one-dimensional random walks with both periodic and fixed boundary conditions [10]. In a one-dimensional chain, the cover-time problem is equivalent to the first-passage time problem, but in higher dimensions the cover-time problem becomes an independent issue. For an m-step search process in a D-dimensional space, it is well known that the area (volume) visited by the walker is $S_m \sim m^{1/2}$ for $D = 1$, and $S_m \sim m/\ln m$ for $D = 2$, $S_m \sim m$ for $D > 2$ [10]. However, the question of how long a walker needs to cover an N-site lattice is not the inverse problem of the previous one. In particular, let t_N be the N-site lattice cover time; it is found that $t_N \sim N^2$ for $D = 1$, $t_N \sim N\ln^2 N$ for $D = 2$, and $t_N \sim N \ln N$ for $D \geqslant 3$ with N going to infinity [11,12]. For $D = 2$, the asymptotic behavior of the random walk cover-time problem was considered on a torus as well [13]. Partial cover time is the time that a random walker visits a given fraction of area, and random cover time is the time to visit a fraction of area previously chosen at random. They are related [14–17] and they have both been discussed in one dimension [14–16] and higher dimensions [17]. Related topics were studied, such as the probability that a site is the last one to be visited, and how long does a walker visit one specific site k times [18].

In this paper, we shall focus on the full cover process, where all sites are visited at least once. Cover time obviously depends on the type of random walks and space dimension. For instance, a Lévy walk is more efficient than Brownian motion in a two-dimensional (2D) searching process. Surprisingly, Chupeau *et al.* recently found that cover times of non-compact explorations, e.g., three-dimensional (3D) Brownian, 2D or 3D Lévy walk, persistent random walk, etc., have a universal distribution [8]. With periodic boundary conditions, the time τ that a noncompact random walker takes to visit all

*huangl@lzu.edu.cn

N sites satisfies the distribution [8]

$$P(x) \sim \exp[-x - \exp(-x)], \tag{1}$$

where

$$x = \frac{\tau}{\langle T \rangle} - \ln N, \tag{2}$$

and $\langle T \rangle$ is the global mean first-passage time, i.e., the mean first-passage time (MFPT) of all directional pairs of sites t and s. MFPT is an important characteristic of random walk. It is the expected time that a random walker first arrives target site t from site s by averaging over all possible paths $\langle T_{t \leftarrow s} \rangle$. This characteristic has been investigated exclusively in previous works [19–23]. The numerical results of the cover-time distribution are in good agreement with Eq. (1) [8]. However, the real diffusion (exploration) process could be much more complex than simple random walk models, such as diffusion of granular matter in a vibrated environment.

Dilute granular systems are regarded as granular gases, and interactions between particles are inelastic so that in each collision some energy is lost. Energy dissipation in granular gases leads to a homogeneous cooling state of which mean square displacement (MSD) can be precisely calculated by means of the Chapman-Enskog method [24,25], and particles perform an extremely compact diffusion. Moreover, this kind of model was used for discussing the ergodicity in granular diffusions [26]. For the nonequilibrium steady state of particles driven by a vibration table, some interesting velocity distributions have been discovered in simulations and experiments [27–29]. From these results, the velocity distribution includes a low-velocity Gaussian core and a high-velocity tail described by exponential functions. In Ref. [30], it is found that in certain cases the velocity distribution can be fitted to a mixture of two non-Gaussian distributions.

Diffusion in granular gases is complicated and quite different from the anomalous diffusion models [31,32]. Therefore, it is important to examine whether the universal rule Eq. (1) is applicable to realistic diffusion processes in granular gases. In this paper, we present results of cover-time distribution from three experiments (I, II, III) under different circumstances. The random walk derived from the original data do not satisfy the noncompactness and periodic boundary condition required by the theory [8]; thus the cover-time distribution does not follow the universal rule. However, after neglecting the data around the edges, which can be regarded as a surface-mediated process [33,34] that makes the equivalent random walk less compact, and applying an approximation method for periodic boundary conditions, the cover-time distribution converges to the universal rule, especially for long cover times.

The following parts of the paper are organized as follows. Section II describes the experimental setup and the treatment for cutting edges (removing the trajectory data close to edge) and applying the periodic boundary approximation. Section III shows the results for the three experiments. A conclusion is provided in Sec. IV.

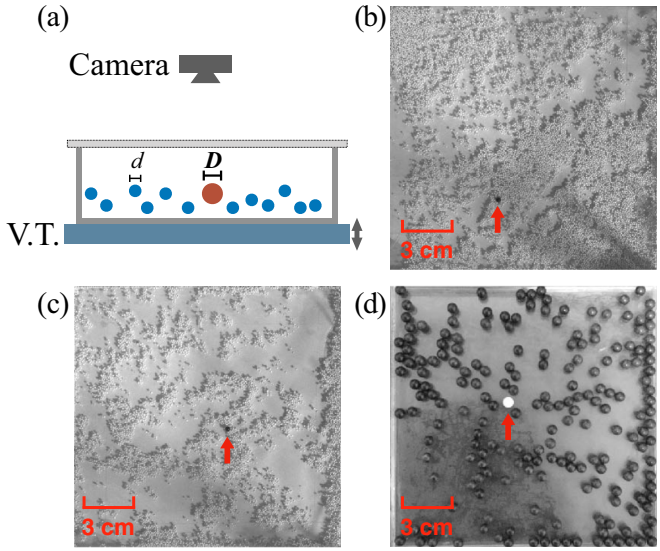

FIG. 1. (a) The schematic diagram of the experimental apparatus. The vibration table is marked by V.T. in the figure. It vibrates in vertical direction with frequency 32 Hz for all three experiments. The high-speed video camera is on top of the container. (b)–(d) Overlook of the three experiments: (I) Brownian motion, (II) low-damping Brownian motion [35–37], and (III) quasi-2D granular diffusion. The particle marked by the red arrow is the tracer particle. The rest of the particles are the granular matter.

II. EXPERIMENTAL SETUP

The schematic diagram of the experimental setup is shown in Fig. 1(a). The container is a cuboid glass box 15 cm long and 15 cm wide. We can adjust the height of the top cover from 1 to 10 cm. In our experiments, the glass container is fixed on a vibration table. One tracer particle with diameter D is put into the container together with the granular particles with average diameter d. The color of the tracer particle is typically in strong contrast to the granular particles. The density of the granular particle can be characterized by the filling rate, which is given by

$$\phi = \frac{n\pi d^2}{4L^2}, \tag{3}$$

where L is the length of the container and n is the number of the granular particles. The vibration table oscillates in vertical direction with amplitude A. In this work, since the results are insensitive to the vibration frequency, we shall fix the frequency at $f = 32$ Hz. The tracer particle's motion is recorded by a high-speed camera from the top. There are 1000×1000 pixels in the field of view. Typical views of the three experiments are shown in Figs. 1(b)–1(d). The detailed parameters are as follows. For experiment I, both the tracer particle and the granular particles are made of ZrO_2, where the average diameter of the granular particles is $d = 1.27$ mm, and the diameter of the tracer particle is $D = 4.2$ mm, the filling rate is $\phi = 0.622$, the height of the container is 10 cm, and the amplitude of vibration is 0.588 mm. For experiment II, the granular particles are the same as that in experiment I, but the tracer particle is different, which is made of Si_3N_4 with diameter $D = 3.0$ mm; the filling rate is decreased to $\phi = 0.15$, the

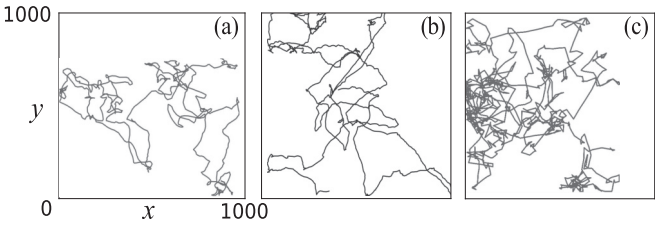

FIG. 2. (a)–(c) Typical trajectories of the tracer particle for experiments I, II, and III, respectively.

amplitude of vibration is changed to 0.27 mm. For experiment III, the tracer particle and the background granular particles are the same and are made of plastic with diameter $D = d = 6.0$ mm, the filling rate is $\phi = 0.226$, the height of the container is 1.5 cm, and the amplitude of vibration is 1.4 mm.

Using a template matching algorithm, we can acquire the position of the tracer particle in every frame of the video. Then the trajectory of the tracer particle is obtained, as exemplified in Fig. 2. For different parameters such as the granular particle density, the vibration amplitude, or the different height of the container, the tracer particle can exhibit different diffusion behaviors [30,32].

The boundary for the tracer particle is fixed; thus one would not expect that the cover-time distribution follows the universal rule in Ref. [8]. Particularly, the tracer particle is more likely to be attracted close to the boundary of the container. A long-time correlation would appear when the tracer moves around the boundaries, and it cannot be neglected by changing to a larger container. Therefore, we propose to take a pretreatment on the original data, i.e., edge cropping and periodic boundary approximation, to reduce the fixed boundary effects, and see if the results will converge to the theory in Ref. [8].

To be specific, in order to eliminate the boundary effect for a container with reasonable size, in the experiments, we cut out the edge region if the distance to the boundary is smaller than parameter l_{cut}, as indicated by the shaded part in Fig. 3, and the trajectory that the particle moves in the edge region is neglected, i.e., the clock is stopped when the tracer particle enters the shaded edge region, and is started again when the particle reenters the central region. To obtain as many covering trajectory samples and full-covering events as possible, and also to approximate the periodic boundary condition, the central region of the container is divided into M blocks ($M = 1$ or 4) with the same size, as shown in Fig. 3. These blocks are regarded to be equivalent, that is, the tracer's trajectory can be translated into one block. To examine the cover-time distribution, the view field needs to be coarsened into a much smaller system to balance between efficiency and precision. Specifically, this block is discretized into 9×9 or 20×20 grids. When the center of the tracer moves into one grid, this grid is regarded to be visited by the tracer. The time that all grids are visited is the full cover time τ. With the experimentally obtained trajectory of the tracer particle, the first-passage time for each pair of grid sites can be measured, and then the global mean first-passage time $\langle T \rangle$ can be determined by averaging the measured first-passage times for all pairs. With Eq. (2), the corresponding x value can be calculated. Assume there are $\widetilde{N}$ full covering events for the whole experimental period, discretizing the x axis with a step δ; then if in $[x - \delta/2,\ x + \delta/2]$ there are k events, the probability function $P(x)$ can be approximated by $k/\widetilde{N}/\delta$. Considering k following the binomial distribution, the uncertainty of $P(x)$ will be around $\sqrt{k(\widetilde{N} - k)/\widetilde{N}^3}/\delta$.

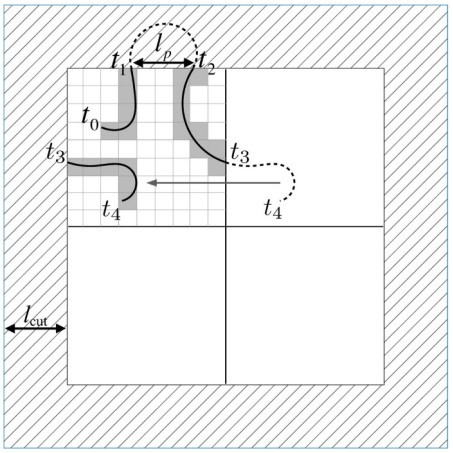

FIG. 3. Schematic of the treatment to the trajectory data to approximate the noncompact random walk. The shaded part is regarded as the edge region, and the width l_{cut} is between 0 and 200 pixels. To remove the fixed boundary effect, the trajectory in the edge region such as $t_1 \to t_2$ is excluded for the covering process statistics. The central region is equally divided into M blocks ($M = 1$ or 4), which are regarded as equivalent, that the trajectories in different blocks can be translated into one block, e.g., $t_3 \to t_4$, and do the cover-time statistics. For $M > 1$, i.e., $M = 4$, this procedure approximates the periodic boundary.

Theoretically, there are three requirements for the cover-time distribution to follow Eq. (1): noncompact random walk, periodic boundary condition, and large N [8]. However, in realistic cases, the parameters should be chosen properly to lie in an intermediate range to reasonably satisfy all these requirements. In particular, the grids in a block cannot be divided too fine to obtain large N. Firstly, the tracker's position given by the template matching algorithm may have uncertainties of a few pixels; thus if the grids are too fine to be comparable with the uncertainties, it could generate fake movements between adjacent grids. Secondly, more grids need a longer cover time, which could significantly reduce the number of full covering events in the limited experimental time. Our results indicate that a 5×5 grid already shows reasonable agreements with the theory. Empirically, a square lattice with 9×9 grids and periodic boundary condition is large enough for checking the cover-time distribution of the random walk model from experimental data, which shows good agreement with Eq. (1) when $l_{\text{cut}} = 200$ and $M = 4$ (Fig. 5). In addition, a 20×20 grid is also used to check the validity of the results when varying the discretized grid size, which exhibits similar results as that for the 9×9 grid. However, increasing the grid size further, say, to 40×40, then our experimental data is not long enough to have reliable statistics.

In principle, for a large enough container, its bottom can be divided into more blocks that the tracer particle's trajectory

would cover one block before the tracer touches the edge region of the container; then a perfect periodic boundary condition might be realized.

III. EXPERIMENTAL RESULTS

A. Results for experiment I: Brownian motion

Brownian motion was first observed in a pollen's movement on the surface of water [38]. The pollen is collided randomly by liquid molecules. The random force leads to Brownian motion of the pollen. In our experiment, the granular matter plays a similar role as the liquid molecules and the tracer particle mimics the pollen. The tracer particle and granular matter are driven by the vibration table in z direction, but in the horizontal direction (x, y-direction), the force only comes from the collision of the tracer with the granular particles, which can be regarded as random forces. When the time interval of the observation is long, the tracer's motion could be Brownian in x and y directions, where the particle's velocity obeys Maxwell distribution:

$$P(v_i) \sim \left(\frac{m\beta_i}{2\pi}\right)^{1/2} e^{-mv_i^2\beta_i/2}, \tag{4}$$

where v_i ($i \in \{x, y\}$) is the tracer's velocity in one direction and m is the tracer's mass. For convenience, we shall use dimensionless quantities for the length (L) and the time (T), which are normalized as follows:

$$l = \frac{L}{\text{spatial resolution}},$$
$$t = \frac{T}{\text{frame duration}}. \tag{5}$$

In this way, both space and time become discretized quantities, with units of pixels and frame duration, respectively. Without loss of generality, we can set $m = 1$. The tracer's velocity distribution in x direction and in y direction both satisfy the Maxwell distribution [Eq. (4)], as shown in Fig. 4(a). The average inverse temperature β_i of the tracer particle in both directions equals 0.11. Furthermore, we have tested different directions, i.e., $y = x$, and the velocities follow the same distribution. During about 100 h of the vibration table experiment, the inverse temperature β_x and β_y are close to each other and stable.

In principle, the mean square displacement of a Brownian motion is proportional to time in all timescales, but in realistic cases such as granular gas, different diffusion behaviors could be observed in different timescales. Figure 4(d) shows the MSD versus time. For very short time intervals (much shorter than the mean free time), we observed ballistic motion $\langle r^2(t)\rangle \propto t^2$. When t is large, there is a good approximation to an ideal Brownian motion $\langle r^2(t)\rangle \propto t$. For an even larger time t, as the system is finite, the MSD becomes saturated. In principle, the characteristic time and the characteristic path length can be estimated by finding the transition point from ballistic or superdiffusion to Brownian motion, which is the cross point of the scaling lines in Fig. 4(d). The root of MSD for the cross point yields the characteristic path length. Although this is feasible for experiment I, there can be big uncertainties for experiments II and III, as the ballistic part in the MSD plot is missing. In the following, we shall demonstrate that the experimental data fits well with the persistent walk model [5] in terms of the distribution function of the excursion displacement. Therefore the characteristic length can be obtained as the average excursion displacement. The two results agree well for experiment I. Therefore we shall use the fitting to persistent walk only to get the characteristic length for experiments II and III.

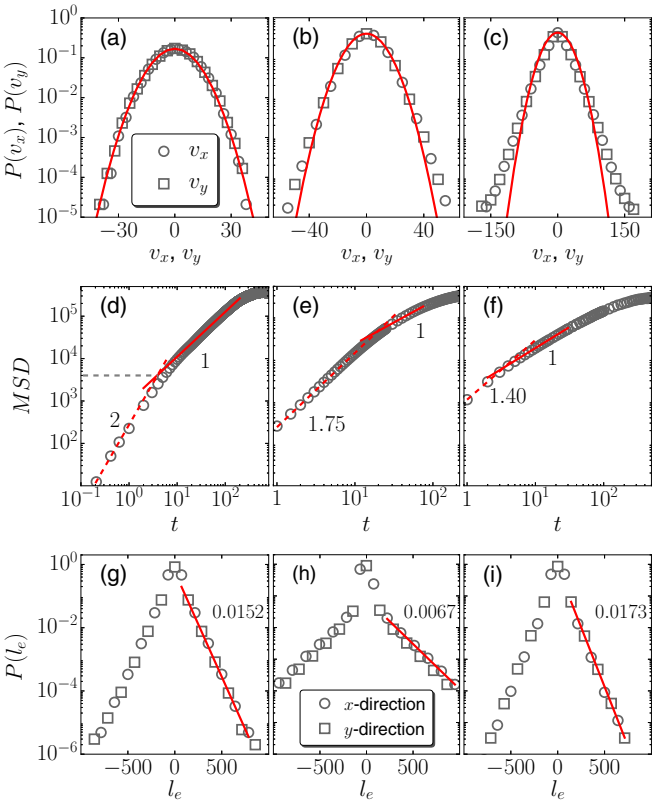

FIG. 4. Characteristics of the random processes in granular gases. The left panels are for experiment I, the middle panels are for experiment II, and the right panels are for experiment III. (a–c) The velocity distribution. The solid red line is fitting to the Maxwell velocity distribution. The circles and squares are experimental results in x and y directions, respectively. The length is normalized by pixel, the spatial resolution of the high-speed camera, and the time is normalized by frame duration. The fitted inverse temperatures are $\beta_x = \beta_y = 0.011$; $v_x = \Delta x/\Delta t$ and $v_y = \Delta y/\Delta t$ are the x and y direction velocity, where $\Delta t = 1$, i.e., one time unit which is the duration between two adjacent camera frames, which is 1/25 s; and Δx and Δy are the displacement in x and y direction in one time unit, respectively. Note that both time and length are dimensionless as normalized in Eq. (5). (d–f) Mean square displacement (MSD). The lines are fitting to the data. (g–i) The distribution of the excursion length l_e. The resulting characteristic lengths for the three experiments are 66, 149, and 58 pixels, respectively.

In a sparse granular gas, a particle always has a nonzero autocorrelation time, i.e., a particle prefers to keep its moving direction for a while before it changes, and this behavior is usually described by the persistent walk model [5]. The probability distribution of the excursion displacement l_e, i.e., the displacement before it changes direction (which are the four directions x, $-x$, y, and $-y$ in our case), follows an

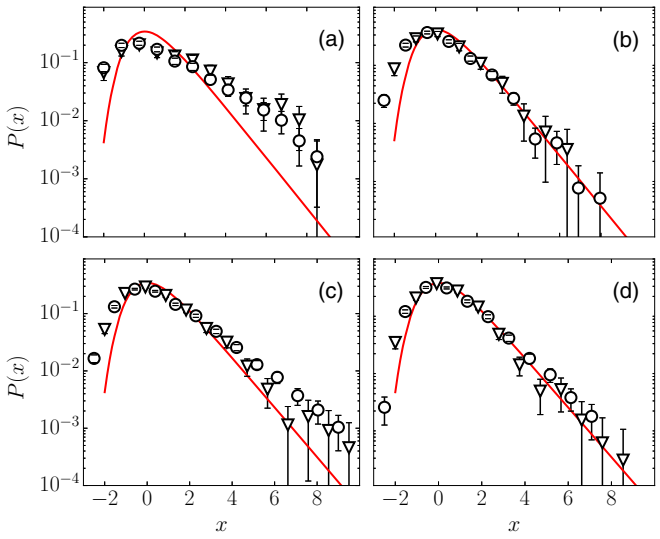

FIG. 5. Cover-time distribution of the random process of the tracer particle in experiment I as in Fig. 3 but with different parameters: (a) $l_{\rm cut} = 0$ and $M = 1$; (b) $l_{\rm cut} = 200$ and $M = 1$; (c) $l_{\rm cut} = 0$ and $M = 4$; (d) $l_{\rm cut} = 200$ and $M = 4$. The block is discretized into 9×9 or 20×20 grids. The circles are experimental results for 9×9 grids, and the triangles are results for 20×20 grids. The red solid curves are the universal law Eq. (1).

exponential function form $P(l_e) \sim \exp(-\gamma|l_e|)$, as shown in Figs. 4(g)–4(i) for the three experiments, where γ is a fitting parameter. The characteristic length is thus given by $1/\gamma$. Note that minus l_e indicates the $-x$ or $-y$ direction. For experiment I, the characteristic length obtained in this way is 66 pixels, while from the MSD curve it is 63 pixels, which agrees with each other well.

In this experiment, the characteristic time is around four frame durations (4/25 second), and the characteristic path length is around 66 pixels (0.99 cm). Thus, even though in large scale the tracer's motion is Brownian (normal diffusion), in local grid coordinates, since the grid length (33 pixels for 9×9 grids, 15 pixels for 20×20 grids) is smaller than the characteristic path length, the motion of the tracer particle from one grid to another is not a completely random walk but something between random walk and ballistic or superdiffusion, introducing local spatial correlations between subsequent movements.

Due to the fixed boundary, the tracer particle stays in the edge region with a higher probability [39]. To systematically investigate the boundary effects, we consider four different cases, as Fig. 5 shows. First, we set $l_{\rm cut} = 0$, discretize the whole region into 9×9 or 20×20 grids ($M = 1$), and calculate the cover time. The results are shown in Fig. 5(a). The cover-time distribution deviates significantly from the theoretical predictions for noncompact random processes. Second, we cut 200 pixels ($l_{\rm cut} = 200$) along the boundary, discretize the remaining region into 9×9 or 20×20 grids ($M = 1$), and calculate the cover time. The distributions are shown in Fig. 5(b). The results get closer to the theoretical prediction, especially when the cover time is large. But when the cover time is small (negative x), the deviation is still apparent. Third, we set $l_{\rm cut} = 0$ but carry out the periodic boundary approximation ($M = 4$), as explained in Fig. 3. The results are shown in Fig. 5(c). As compared with Fig. 5(b), the deviation becomes larger. This indicates that cutting the edge region is more efficient in approximating the situation assumed in the theoretical prediction [8], especially for slow covering processes. Fourth, we set $l_{\rm cut} = 200$ and carry out the periodic boundary approximation ($M = 4$). The results are shown in Fig. 5(d). Now the experimental results agree with the universal law well.

B. Results for experiments II and III: Non-Brownian motion specific to the granular materials

To verify the validity of the universal law in more general circumstances, we have carried out two more sets of experiments (II and III), which are unique to random processes in vibrated granular materials. Experiment II is for Brownian motion with low damping [40], and experiment III is for unusual diffusion in a quasi-2D granular gas [30].

In experiment II, the granular particles and the container are the same as in experiment I; the difference from experiment I is that the filling rate of granular matter ϕ is decreased to 0.15, much sparser than experiment I, thus the ballistic motion is more dominant. The tracer particle is made up by silicon nitride (Si_3N_4) with diameter $D = 3$ mm. It is much larger and heavier than the granular particles ($d = 1.27$ mm ZrO_2). The vibration amplitude is decreased to 0.27 mm. The total time for the experiment with effective data is over 110 h. The speed of the tracer particle in this case is faster. The characteristic path length is 149 pixels, which is much larger than the size of a grid (33 pixels for 9×9 grids, 15 pixels for 20×20 grids) when 200 pixels near the boundary are cut out. Thus in this case the damping effect for the tracer particle is less severe.

In this experiment the velocity distribution of the tracer particle slightly deviates from Maxwell distribution Eq. (4) in the high-speed regime, but it still contains a Gaussian core when the speed is small [see Fig. 4(b)]. Also, the frame rate used in our experiment is not high enough to caption the short-time ballistic motion of the tracer particle; therefore the MSD plot [Fig. 4(e)] lacks the ballistic part. For the excursion displacement distribution Fig. 4(h), different from the other two experiments, there seems to be two distinct characteristic lengths, as it is a mixture of two exponential curves, with one being 149 pixels and the other much smaller.

Experiment III is for dilute quasi-2D granular gas. The granular particles are made of plastics, whose diameter is 6 mm and the standard deviation is 0.09 mm. The tracer particle is chosen to be the same as the granular particle but painted in a different color. The filling rate is $\phi = 0.226$. The vibration amplitude is 1.4 mm. The container is covered with a height of only 1.5 cm; thus the particle's motion is mostly confined in the (x, y) plane.

Generally, the microdynamics of diffusion for a single particle is described by continuous time random walk (CTRW) theory [32]. It is supposed that a random walk process can be split into two parts—waiting and jumping—and the type of diffusion depends on the convergence or divergence of waiting time and jumping length. It is common for quasi-2D dilute granular gases to display a similar but not exactly the same behavior to what CTRW describes. For instance,

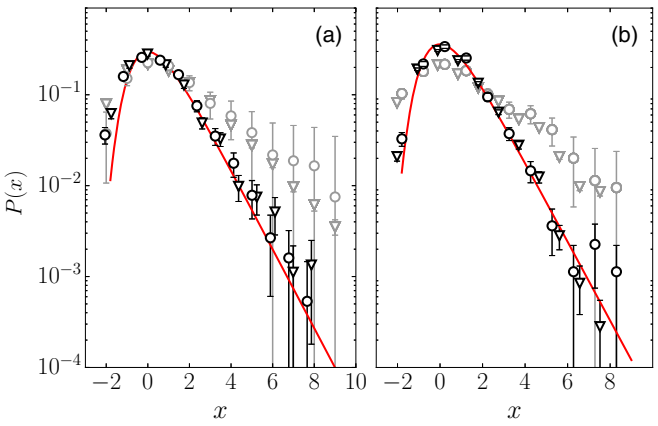

FIG. 6. Cover-time distribution for experiments II [panel (a)] and III [panel (b)]. Gray symbols are for $l_{\rm cut} = 0$ and $M = 1$; black symbols are for $l_{\rm cut} = 200$ and $M = 4$. Circles are results for 9×9 grids, and triangles are results for 20×20 grids. The red solid curves are Eq. (1).

velocity distributions in quasi-2D dilute granular gases could be highly non-Maxwellian [41] because it consists of two types of collision [30]: collision with the top or the bottom of the container and collision with other particles. The former type of collision, considering the roughness of the top or bottom, imposes a small and random velocity in horizontal direction. Because of friction, the velocity could also be reduced. For the latter type of collision, the tracer particle gains a high speed by interacting with other particles. The two types of collisions could occur alternately and together shape the velocity distribution for the tracer particle. In fact, it is observed that the particle velocity distribution is a piecewise exponential function [41], which almost has no Gaussian core [see also Fig. 4(c)]. Since the velocity is much larger, the exponent of the fitting to the MSD in the small t limit is even smaller [Fig. 4(f)]. The excursion length distribution has a perfect exponential form and yields a characteristic path length of 58 pixels, which is also larger than the size of a grid.

The cover-time distributions for both experiments II and III are shown in Fig. 6. Similar to experiment I, without cutting edge and periodic boundary approximations, the results deviate from the universal law significantly. After cutting the trajectories close to the boundary and applying the periodic boundary approximations, the cover-time distribution shows good agreement with the theoretical prediction. Even still, there are cases that the cover-time probability is slightly higher than the theory [Eq. (1)], especially for rapid cover processes ($x < 0$), which persists for all three experiments.

IV. CONCLUSION

To conclude, we have carried out granular gas experiments to investigate whether the random processes in this system satisfy the universal cover-time distribution proposed in Ref. [8]. For different parameters of the system, such as the size and material of the granular particles and the tracer particle, the filling rate, the vibration amplitude, etc., the motion of the tracer particle can be quite different. Interestingly, the excursion length distribution follows an exponential function form for all three experiments, suggesting that the persistent random walk model [5] captures a general feature of granular gases, although in experiment II there seems to be two distinct characteristic length scales. The direct cover-time analysis by discretizing the random processes of the tracer particle into 9×9 or 20×20 grids indicates a large deviation from the universal law, which can be understood in that the realistic random motion of the tracer particle does not satisfy the ideal assumptions for the theory, such as the attracting effect at the boundary and the nonperiodic boundary condition due to the fixed boundaries. To remove the boundary effect, we proposed to neglect the trajectories of the tracer particle if it is too close to the boundary, say, $l_{\rm cut}$, and then do the cover-time statistics for the central region. This results in an equivalent surface-mediated process [33,34] that makes the random walk less compact. Furthermore, the central region can be divided into four blocks, where they are regarded to be equivalent to mimic the periodic boundary condition, i.e., the trajectories in other blocks are translated back to one particular block, and also to increase the number of full cover events for better statistics. As a result, after removing the edge region and applying the periodic boundary approximation, the cover-time distribution agrees with the universal law quite well for all three experiments. During this process, it is also found that the attracting boundary effect is more dominant in causing the discrepancy from the universal law, especially for long cover-time processes. Periodic boundary approximation helps the statistics to agree better with the universal law in the fast covering process. Our work opens the way to new tests of the theoretical law Eq. (1) [8] and of its limits, and also renews interest for a theoretical description of the distribution of cover times with fixed boundary conditions, and in compact situations.

ACKNOWLEDGMENTS

We would like to thank the anonymous reviewers for their constructive comments. This work was supported by NNSF of China under Grants No. 11422541 and No. 11775101.

K.C. and J.-Q.D. have contributed equally to this work.

[1] K. Pearson, Nature (London) **72**, 294 (1905).

[2] F. Spitzer, *Principles of Random Walk* (Springer Science Business Media, New York, 2013), Vol. 34.

[3] P. Lévy, *Theorie de L'addition Des Variables Aleatoires* (Gautheir-Villars, Paris, 1937).

[4] R. Fürth, Z. Phys. **2**, 244 (1920).

[5] V. Tejedor, R. Voituriez, and O. Bénichou, Phys. Rev. Lett. **108**, 088103 (2012).
[6] E. W. Montroll, J. Chem. Phys. **18**, 734 (1950).
[7] O. Bénichou, C. Chevalier, J. Klafter, B. Meyer, and R. Voituriez, Nat. Chem. **2**, 472 (2010).
[8] M. Chupeau, O. Bénichou, and R. Voituriez, Nat. Phys. **11**, 844 (2015).
[9] J. D. Kahn, N. Linial, N. Nisan, and M. E. Saks, J. Theor. Probab. **2**, 121 (1989).
[10] A. M. Nemirovsky, H. O. Mártin, and M. D. Coutinho-Filho, Phys. Rev. A **41**, 761 (1990).
[11] M. J. A. M. Brummelhuis and H. J. Hilhorst, Physica A **185**, 35 (1992).
[12] C. S. Yokoi, A. Hernández-Machado, and L. Ramírez-Piscina, Phys. Lett. A **145**, 82 (1990).
[13] A. Dembo, Y. Peres, J. Rosen, and O. Zeitouni, Ann. Math. **160**, 433 (2004).
[14] M. S. Nascimento, M. D. Coutinho-Filho, and C. S. O. Yokoi, Phys. Rev. E **63**, 066125 (2001).
[15] M. Chupeau, O. Bénichou, and R. Voituriez, Phys. Rev. E **89**, 062129 (2014).
[16] P. C. Hemmer and S. Hemmer, Physica A **251**, 245 (1998).
[17] K. R. Coutinho, M. D. Coutinho-Filho, M. A. F. Gomes, and A. M. Nemirovsky, Phys. Rev. Lett. **72**, 3745 (1994).
[18] C. R. Mirasso and H. O. Mártin, Z. Phys. B–Condens. Mat. **82**, 433 (1991).
[19] M. Yang, D.-J. Wu, and L. Cao, Commun. Theor. Phys. **23**, 167 (1995).
[20] I. Eliazar and J. Klafter, Physica A **336**, 219 (2004).
[21] R. C. Lua and A. Y. Grosberg, Phys. Rev. E **72**, 061918 (2005).
[22] J. D. Noh and H. Rieger, Phys. Rev. Lett. **92**, 118701 (2004).
[23] S. Condamin, O. Bénichou, and M. Moreau, Phys. Rev. E **75**, 021111 (2007).
[24] N. V. Brilliantov and T. Pöschel, Chaos **15**, 026108 (2005).
[25] N. V. Brilliantov and T. Pöschel, Phys. Rev. E **61**, 1716 (2000).
[26] A. Bodrova, A. V. Chechkin, A. G. Cherstvy, and R. Metzler, Phys. Chem. Chem. Phys. **17**, 21791 (2015).
[27] J. S. van Zon and F. C. MacKintosh, Phys. Rev. E **72**, 051301 (2005).
[28] J. M. Montanero and A. Santos, Granular Matter **2**, 53 (2000).
[29] B. Wang, J. Kuo, S. C. Bae, and S. Granick, Nat. Mater. **11**, 481 (2012).
[30] W. Chen and K. To, Phys. Rev. E **80**, 061305 (2009).
[31] R. Metzler, J.-H. Jeon, A. G. Cherstvy, and E. Barkai, Phys. Chem. Chem. Phys. **16**, 24128 (2014).
[32] R. Metzler and J. Klafter, Phys. Rep. **339**, 1 (2000).
[33] O. Bénichou, D. Grebenkov, P. Levitz, C. Loverdo, and R. Voituriez, Phys. Rev. Lett. **105**, 150606 (2010).
[34] O. Bénichou, D. Grebenkov, P. Levitz, C. Loverdo, and R. Voituriez, J. Stat. Phys. **142**, 657 (2011).
[35] H. Safdari, A. G. Cherstvy, A. V. Chechkin, A. Bodrova, and R. Metzler, Phys. Rev. E **95**, 012120 (2017).
[36] M. S. Simon, J. Sancho, and K. Lindenberg, Eur. Phys. J. B **87**, 201 (2014).
[37] A. S. Bodrova, A. V. Chechkin, A. G. Cherstvy, H. Safdari, I. M. Sokolov, and R. Metzler, Sci. Rep. **6**, 30520 (2016).
[38] R. Brown, Philos. Mag. **4**, 161 (1828).
[39] Y.-Z. Chen, Z.-G. Huang, and Y.-C. Lai, Sci. Rep. **4**, 6121 (2014).
[40] S. K. Ghosh, A. G. Cherstvy, and R. Metzler, Phys. Chem. Chem. Phys. **17**, 1847 (2015).
[41] C. Scholz and T. Pöschel, Phys. Rev. Lett. **118**, 198003 (2017).